Least-squares migration/inversion of blended data

Yaxun Tang and Biondo Biondi

ABSTRACT

We present a method based on least-squares migration/inversion to directly image data collected from recently developed wide-azimuth acquisition geometries, such as simultaneous shooting and continuous shooting, where two or more shot records are often blended together. We show that by using least-squares migration/inversion, we not only enhance the resolution of the image, but more importantly, we also suppress the crosstalk or acquisition footprint, without any pre-separation of the blended data. We demonstrate the concept and methodology in 2-D and apply the data-space inversion scheme to the Marmousi model, where an optimally reconstructed image, free from crosstalk artifacts, is obtained.

INTRODUCTION

High-quality seismic images are extremely important for subsalt exploration, but data collected from conventional narrow-azimuth towed streamers (NATS) often produce poor subsalt images due to insufficient azimuth coverage. Recently developed wide-azimuth towed streamers (WATS) (Michell et al., 2006) and multi-azimuth towed streamers (MATS) (Keggin et al., 2006; Howard and Moldoveanu, 2006) acquisition technologies have greatly improved subsalt illumination, and hence better subsalt images are obtained. However, acquiring marine WATS or MATS data is expensive. One main reason is the inefficiency of the conventional way of acquiring data, which requires waiting long enough between shots to prevent interference (Beasley et al., 1998; Beasley, 2008; Berkhout, 2008). As a consequence, the source domain is often poorly sampled to reduce the survey time.

To gain efficiency, simultaneous shooting (Beasley et al., 1998; Beasley, 2008; Hampson et al., 2008) and continuous shooting, or more generally, blended acquisition geometry (Berkhout, 2008), have been proposed to replace the conventional shooting strategy. In the blended acquisition geometry, we try to keep shooting and recording continuously, so that waiting between shots is minimized and a denser source sampling can be obtained. However, this shooting and recording strategy results in two or more shot records blending together and brings processing challenges. A common practice for processing these blended data is to first separate the blended shot gathers into individual ones in the data domain (Spitz et al., 2008; Akerberg et al., 2008), called "deblending" by Berkhout (2008). Then conventional processing flows are applied to

these deblended shot gathers. The main issue with this strategy is that it can be extremely difficult to separate the blended gathers when the shot spacing is close and many shots are blended together.

In this paper, we present an alternative method of processing these blended data sets. Instead of deblending the data prior to the imaging step, we propose to directly image them without any pre-separation. The simplest way for direct imaging would be migration; however, migration of blended data generates images contaminated by crosstalk. The crosstalk is due to the introduction of the blending operator (Berkhout, 2008), which makes the corresponding combined Born modeling operator far from unitary; thus its adjoint, also known as migration, gives poor reconstruction of the reflectivity. A possible solution is to go beyond migration by formulating the imaging problem as a least-squares migration/inversion (LSI) problem, which uses the pseudo-inverse of the combined Born modeling operator to reconstruct the reflectivity of the subsurface.

We extend the LSI theory from the conventional acquisition geometry (Nemeth et al., 1999; Clapp, 2005; Valenciano, 2008; Tang, 2008b) to the blended acquisition geometry and develop inversion schemes in both data space and model space. The former minimizes a data-space defined objective function, while the latter minimizes a model-space defined objective function. By comparing the pros and cons of both inversion schemes, we show that the data-space approach is preferred over the model-space approach if the combined Born modeling operator is far from unitary; that is, its normal operator, the Hessian, has many non-negligible off-diagonal elements. Hence an approximate Hessian with a limited number of off-diagonal elements cannot capture the characteristics of the crosstalk, making it less effective in removing the crosstalk in the model space. Big Hessian filters, which sufficiently capture the information of the crosstalk, are too expensive for practical applications. Therefore, the data-space inversion approach, which does not require explicitly computing the Hessian, becomes more attractive. We demonstrate our ideas with simple synthetic examples, and we also test the data-space inversion scheme on the Marmousi model to illustrate how the crosstalk is suppressed through inverting the combined Born modeling operator. Application to 4-D (time-lapse) inversion using blended data sets is discussed in a companion paper by Ayeni et al. (2009).

This paper is organized as follows: we first describe the problem of directly imaging the blended data through migration; then we develop the theory of LSI in both data space and model space for blended data, and compare the pros and cons of the two domains for imaging blended data. Finally, we apply the data-space inversion approach to the Marmousi model to test its performance on a complex model.

PROBLEMS WITH DIRECT MIGRATION

Within limits of the Born approximation of the acoustic wave equation, the seismic data can be modeled with a linear operator as follows:

$$\mathbf{d} = \mathbf{L}\mathbf{m}, \tag{1}$$

where $\mathbf{d}$ is the modeled data, $\mathbf{L}$ is the forward Born modeling operator, and $\mathbf{m}$ denotes the reflectivity, a perturbed quantity from the background velocity. Equation 1 models the data for the conventional acquisition geometry, i.e., without interference between different shots. For the blended acquisition geometry, however, two or more shot records are often blended together, creating one or more super-areal shot record(s). This blending process can be described by a linear transform as follows:

$$\widetilde{\mathbf{d}} = \mathbf{B}\mathbf{d}, \tag{2}$$

where $\mathbf{B}$ is the so-called blending (Berkhout, 2008) or encoding (Romero et al., 2000; Tang, 2008a) operator, and $\widetilde{\mathbf{d}}$ is the set of super-areal shot records after blending. Substituting equation 1 into equation 2 leads to the modeling equation for the blended acquisition geometry:

$$\widetilde{\mathbf{d}} = \mathbf{B}\mathbf{L}\mathbf{m} = \widetilde{\mathbf{L}}\mathbf{m}, \tag{3}$$

where $\widetilde{\mathbf{L}} = \mathbf{B}\mathbf{L}$ is defined as the combined Born modeling operator.

There are many choices of the blending operator; which one produces the optimal imaging result might be case-dependent and is beyond the scope of this paper. In this paper, we mainly consider two different blending operators: a linear-time-delay blending operator and a random-time-delay blending operator. The first operator seems to be common and easy to implement in practice for acquiring marine data, while the second one is interesting and has been partially adopted in acquiring both land and marine data with simultaneous shooting (Hampson et al., 2008). For example, Figure 1 shows a scattering reflectivity model with a constant velocity of 2000 m/s. Figure 2 and Figure 3 show the snapshots of the corresponding blended source wavefields. For both cases, 41 point sources with an equal spacing of 100 m are blended into one composite source. Figure 4 shows the modeled blended data. Given the complexity of the super-areal shot gathers shown in Figure 4, it might be very difficult or even impossible to deblend them.

We can directly use the adjoint of the combined modeling operator, which is also widely known as the migration operator, to reconstruct the reflectivity as follows:

$$\widetilde{\mathbf{m}}_{\text{mig}} = \widetilde{\mathbf{L}}'\widetilde{\mathbf{d}}_{\text{obs}} = \mathbf{L}'\mathbf{B}'\mathbf{B}\mathbf{d}_{\text{obs}}, \tag{4}$$

where the superscript $'$ denotes the conjugate transpose and the subscript $_{\text{obs}}$ denotes observed data. Contrary to the imaging formula in conventional acquisition geometry, now we have an extra $\mathbf{B}'\mathbf{B}$ in our imaging formula, which has a direct impact on the imaging quality of blended data. If $\mathbf{B}'\mathbf{B}$ is close to unitary, i.e., $\mathbf{B}'\mathbf{B} \approx \mathbf{I}$ with $\mathbf{I}$ being the identity matrix, then direct migration of blended data would produce exactly

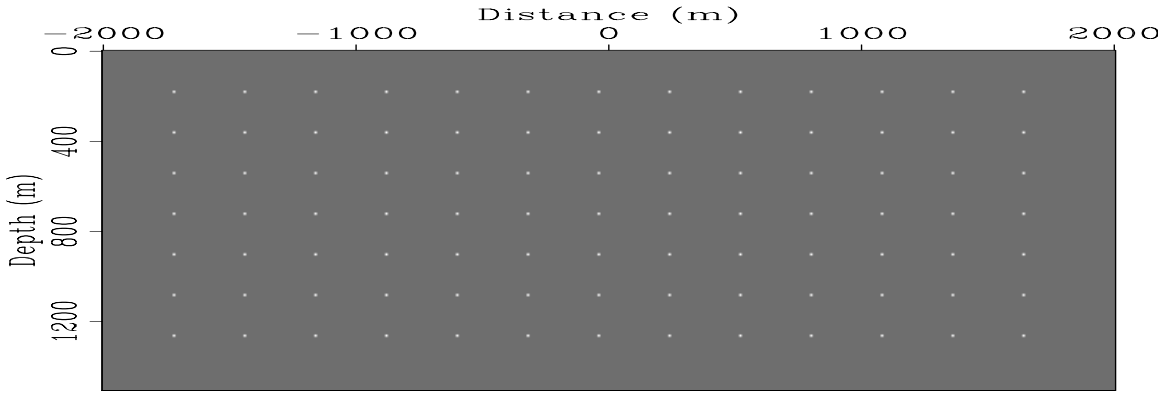

Figure 1: A reflectivity model containing many point scatterers. [**ER**]

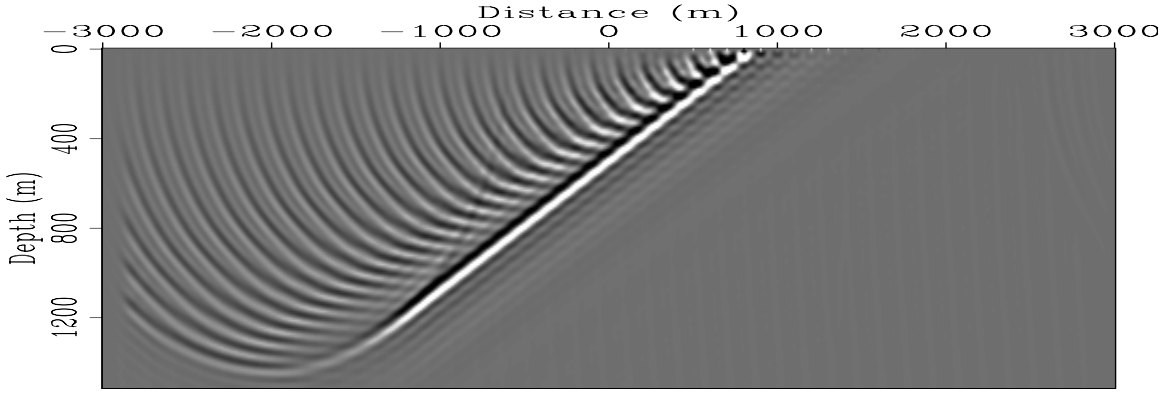

Figure 2: Source wavefield after linear-time-delay blending. [**CR**]

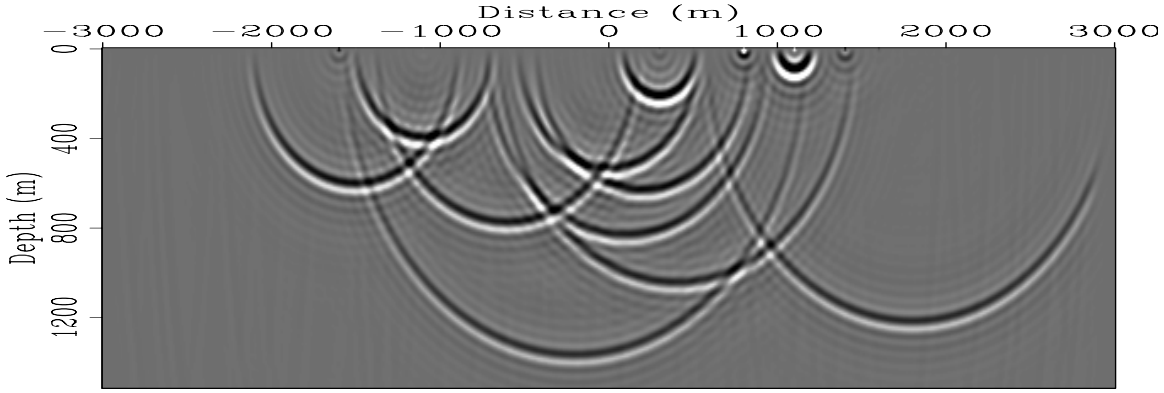

Figure 3: Source wavefield after random-time-delay blending. [**CR**]

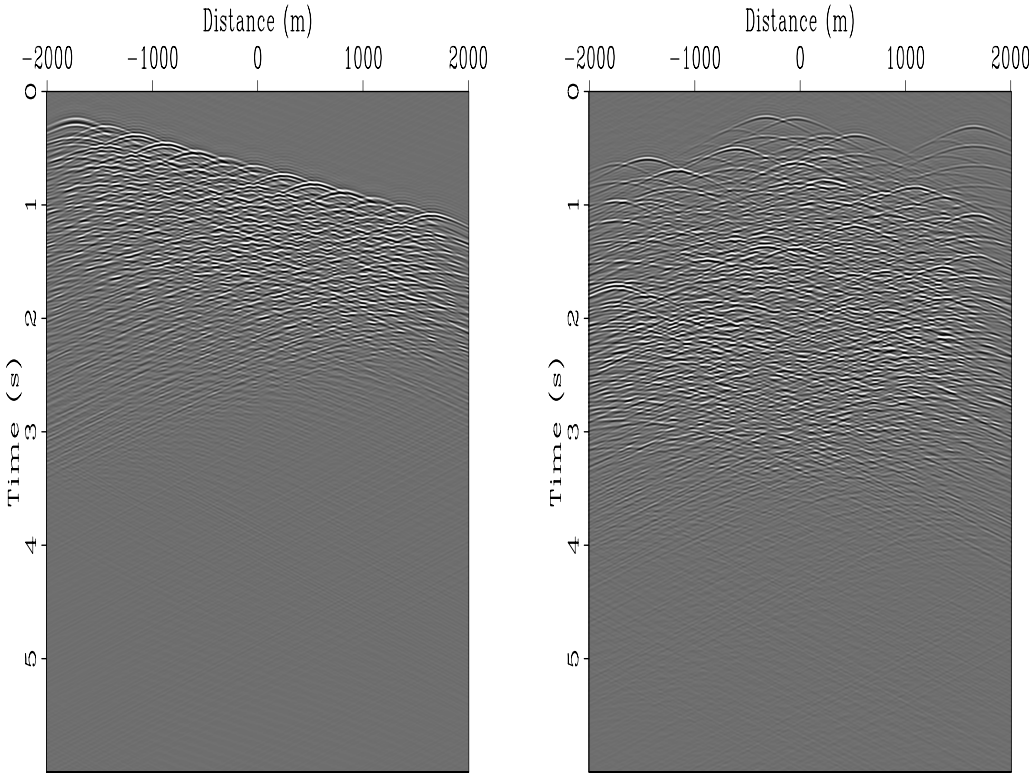

(a) (b)

Figure 4: Modeled blended shot gather. (a) Linear-time delay blending and (b) random-time-delay blending. [**CR**]

the same results as migration of conventional data, and the blending process would produce little impact on the final image we obtain. However, in reality, $\mathbf{B}'\mathbf{B}$ is often far from unitary, because $\mathbf{B}$ is usually a short matrix (its number of rows is much smaller than its number of columns); thus its normal operator, $\mathbf{B}'\mathbf{B}$, is rank deficient. In other words, there are many non-negligible off-diagonal elements in $\mathbf{B}'\mathbf{B}$. As a consequence, direct migration using equation 4 would produce crosstalk artifacts. An example is demonstrated in Figure 5 and Figure 6, which illustrate the migrated images for the blended data shown in Figure 4; the images are severely degraded by the crosstalk artifacts. For comparison, Figure 7 shows the crosstalk-free image by migrating the data synthsized with the conventional acquisition geometry (when $\mathbf{B} = \mathbf{I}$).

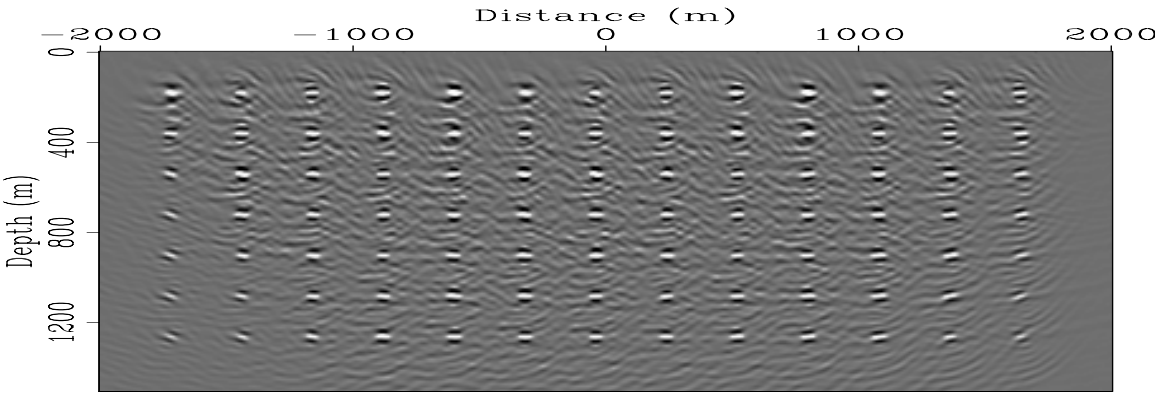

Figure 5: Migration of linear-time-delay blended data. [**CR**]

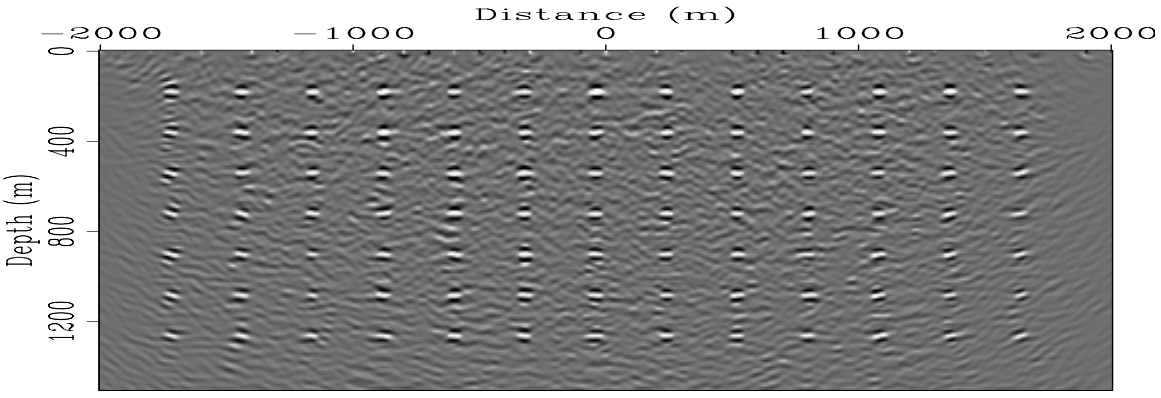

Figure 6: Migration of random-time-delay blended data. [**CR**]

DIRECT IMAGING THROUGH INVERSION

A way to reduce the crosstalk is to go beyond migration by formulating the imaging problem as a LSI problem. The motivation behind LSI is that the pseudo-inverse of the combined modeling operator $\widetilde{\mathbf{L}}$ should be able to optimally reconstruct the reflectivity; hence the image would be minimally affected by the crosstalk artifacts.

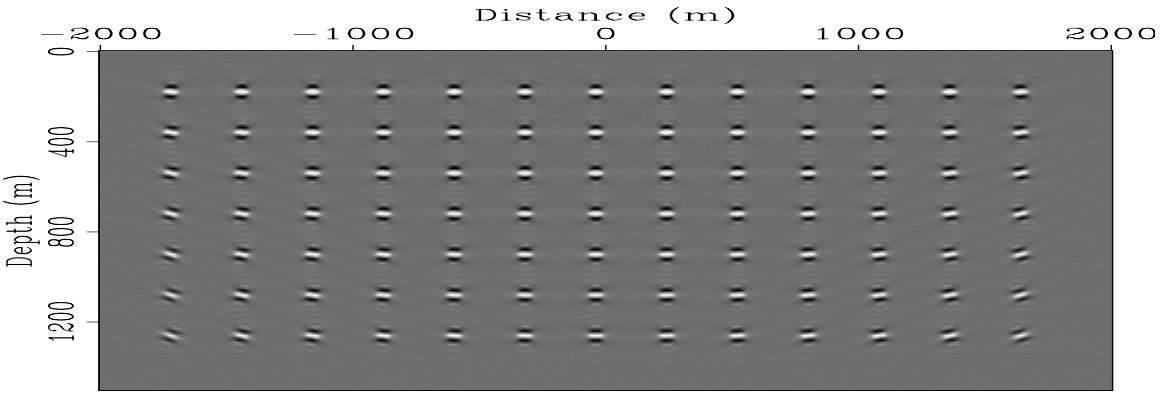

Figure 7: Migration of the data acquired with the conventional acquisition geometry. [**CR**]

The LSI can be performed either in the model space or in the data space, each of which has its own pros and cons. We will analyze both of them for imaging the blended data.

LSI in the model space

The least-squares solution of equation 3 can be formally written as follows:

$$\mathbf{m} = \widetilde{\mathbf{H}}^{-1}\widetilde{\mathbf{L}}'\widetilde{\mathbf{d}}_{\text{obs}} = \widetilde{\mathbf{H}}^{-1}\widetilde{\mathbf{m}}_{\text{mig}}, \tag{5}$$

where $\widetilde{\mathbf{H}} = \widetilde{\mathbf{L}}'\widetilde{\mathbf{L}} = \mathbf{L}'\mathbf{B}'\mathbf{B}\mathbf{L}$ is the Hessian for the blended acquisition geometry. However, equation 5 has only symbolic meaning, because the Hessian is often singular and its inverse is not easy to obtain directly. A more practical method is to reconstruct the reflectivity $\mathbf{m}$ through iterative inverse filtering by minimizing a model-space objective function defined as follows:

$$J(\mathbf{m}) = ||\widetilde{\mathbf{H}}\mathbf{m} - \widetilde{\mathbf{m}}_{\text{mig}}||_2^2 + \epsilon||\mathbf{A}\mathbf{m}||_2^2, \tag{6}$$

where $||\cdot||_2$ stands for the ℓ_2 norm, $\mathbf{A}$ is a regularization operator that imposes prior information that we know about the model $\mathbf{m}$, and ϵ is a trade-off parameter that controls the strength of regularization.

The advantage of the model-space formulation is that it can be implemented in a target-oriented fashion, which can substantially reduce the size of the problem and hence the computational cost (Valenciano, 2008). However, it requires explicitly computing the Hessian operator, which is expensive without certain approximations. As demonstrated by Valenciano (2008), for a typical conventional acquisition geometry, i.e., when $\mathbf{B} = \mathbf{I}$, the Hessian operator $\mathbf{L}'\mathbf{L}$ is diagonally dominant for areas of good illumination, but for areas of poor illumination, the diagonal energy spreads along its off-diagonals. The spreading is limited and can almost be captured by a limited

number of off-diagonal elements. That is why Valenciano (2008) suggests computing a truncated Hessian filter to approximate the exact Hessian for inverse filtering. Doing this makes the cost of the model-space inversion scheme affordable for practical applications. Figure 8(a) shows the local Hessian operator located at $x = 0$ m and $z = 750$ m in the subsurface (a row of the entire Hessian matrix) for the previous scattering model with the conventional acquisition geometry. The origin of this plot denotes the diagonal element of the Hessian, while locations not at the origin denote the off-diagonal elements of the Hessian. As expected, the Hessian is well focused around its diagonal part, and hence can be approximated by a filter with a small size. However, for the blended acquisition geometry, the combined modeling operator $\widetilde{\mathbf{L}}$ becomes far from unitary, and hence the Hessian $\widetilde{\mathbf{H}}$ has non-negligible off-diagonal energy, which can spread over many of the off-diagonal elements. This phenomenon is confirmed by Figure 8(b) and Figure 8(c), which show the local Hessian operators at the same image point for different blended acquisition geometries. It is clear that a filter with a small size could not capture all the important characteristics of the crosstalk in the migrated image; therefore inverse filtering would fail to remove the crosstalk. Figure 9 shows the model-space inversion result with a small Hessian filter (41×41 in size) for both blended acquisition geometries. The crosstalk is not removed at all, and the inverted images become even worse.

For comparison, Figure 10 shows the inversion result with the full Hessian for a model with only one scatterer in the subsurface (the blending parameters are the same as those for the multiple scattering model). The full Hessian includes all possible off-diagonal elements, so it accurately predicts the crosstalk pattern. The inversion successfully removes the crosstalk. However, the full Hessian is too expensive to compute even though it is target-oriented, and the cost of computing many off-diagonals can quickly outweight the achieved savings of performing the inversion in a target-oriented fashion. Therefore, we seek an inversion approach that does not require explicitly computing the Hessian, so that we do not have to worry about the size of the Hessian filter. This important consideration leads us to the following data-space inversion approach.

LSI in the data space

The data-space LSI minimizes the following objective function:

$$F(\mathbf{m}) = ||\widetilde{\mathbf{L}}\mathbf{m} - \widetilde{\mathbf{d}}_{\text{obs}}||_2^2 + \epsilon||\mathbf{A}\mathbf{m}||_2^2. \tag{7}$$

The data-space objective function $F(\mathbf{m})$ can be minimized through gradient-based optimization schemes, which iteratively reconstruct the model parameters. The advantage of this data-space formulation is that it does not require explicitly building the Hessian operator; hence all crosstalk information is captured implicitly. However, the data-space formulation lacks flexibility and can not be implemented in a target-oriented fashion. Its cost is another concern, because each iteration costs about the same as two migrations, making it challenging for large scale applications. The cost

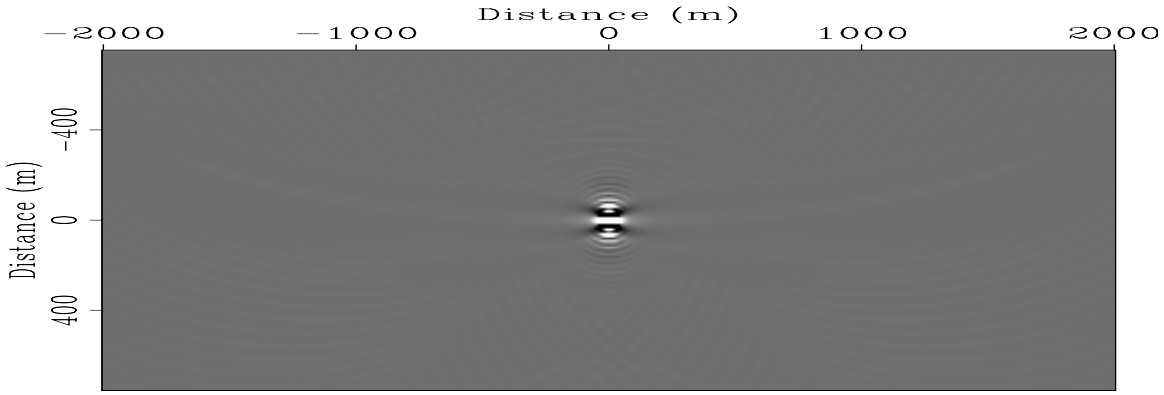

(a)

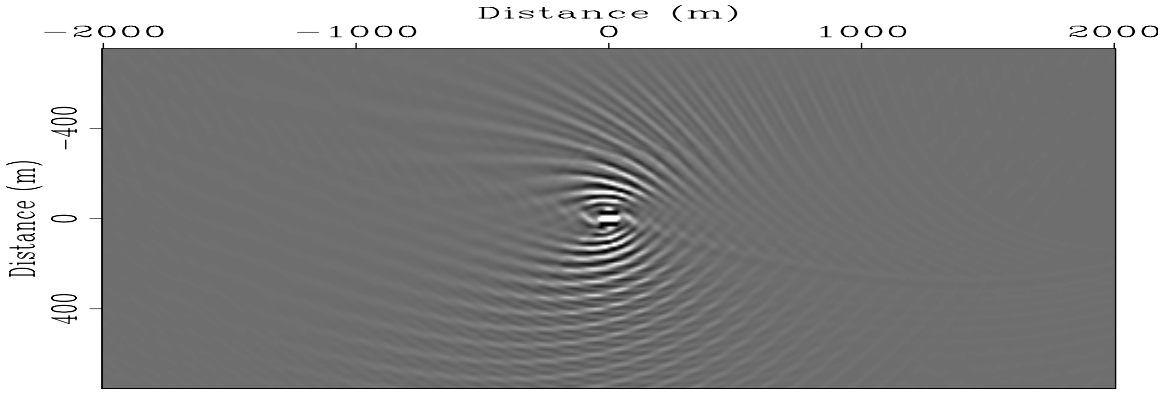

(b)

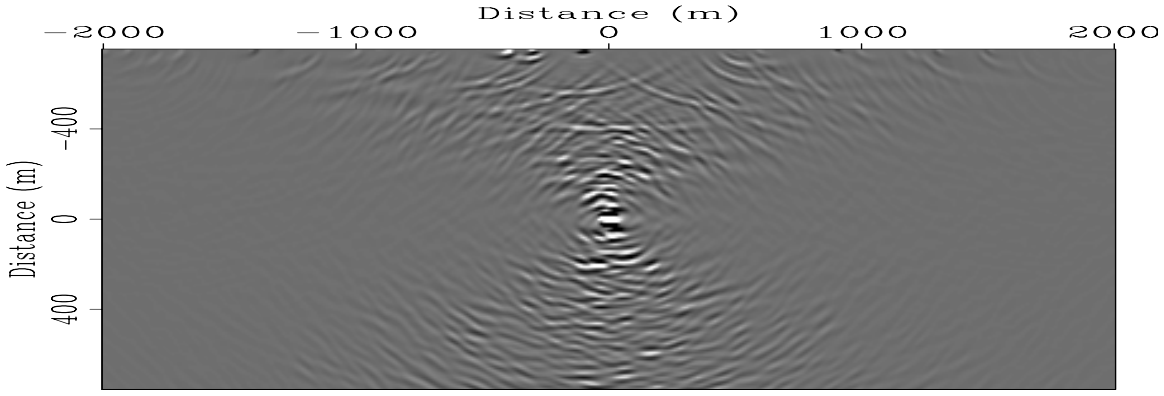

(c)

Figure 8: The local Hessian operator located at $x = 0$ m and $z = 750$ m in the subsurface. (a) Conventional acquisition geometry, (b) linear-time-delay blended acquisition geometry, and (c) random-time-delay blended acquisition geometry. [**CR**]

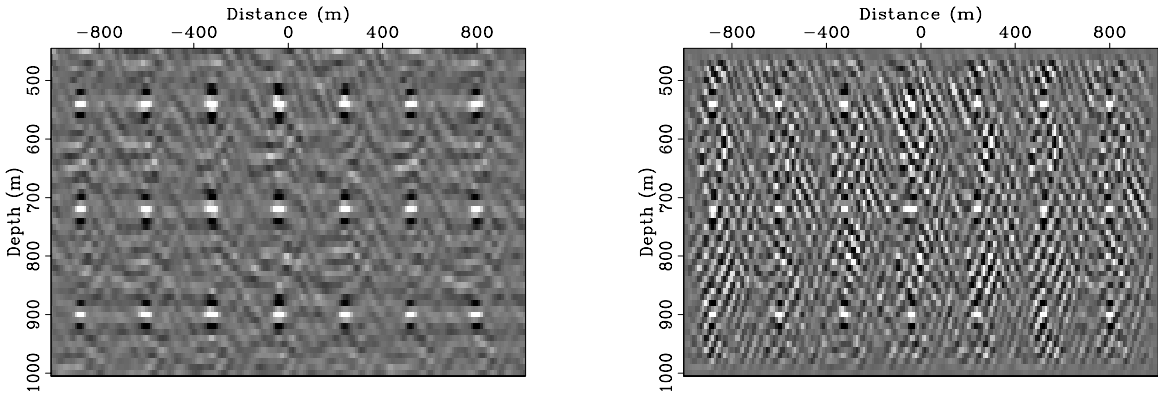

(a)

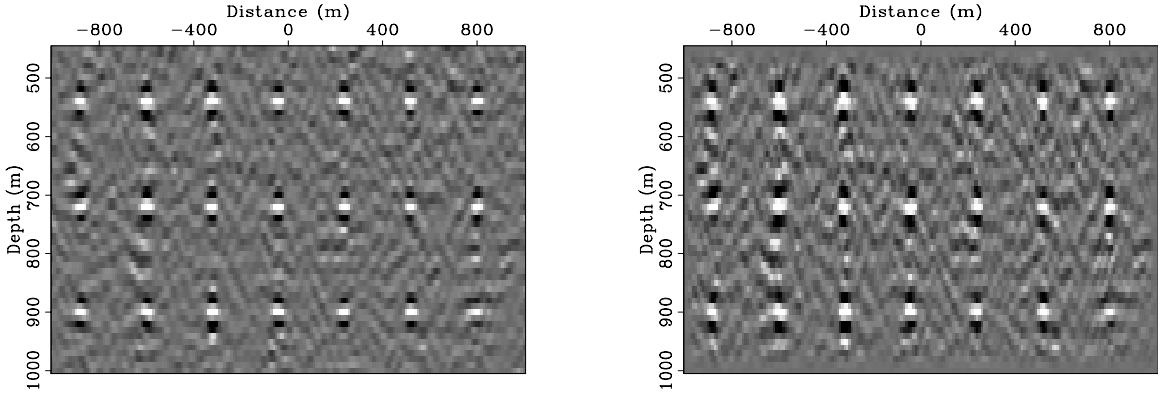

(b)

Figure 9: Comparison between migration and model-space LSI with a small Hessian (41×41 in size) for the model containing multiple scatters. (a) Linear-time-delay blended acquisition geometry and (b) random-time-delay blended acquisition geometry. In both (a) and (b), the left panel shows the migrated result, while the right panel shows the inverted result. [**CR**]

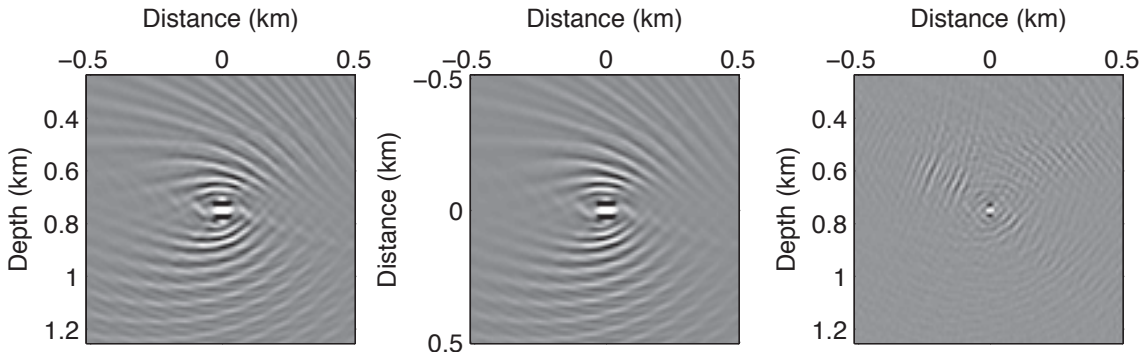

(a)

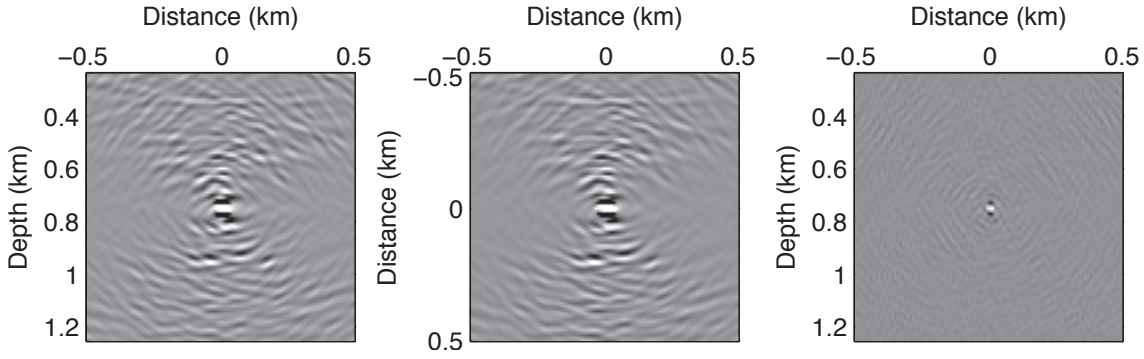

(b)

Figure 10: Comparison between migration and model-space LSI with a full Hessian (401×151 in size) for a single-scatterer model. (a) Linear-time-delay blended acquisition geometry and (b) random-time-delay blended acquisition geometry. In both (a) and (b), the left panel shows the migrated result, the center panel shows the local Hessian operator (a row of the full Hessian), and the right panel shows the inverted result. [**CR**]

can be significantly reduced by using proper preconditioners, which may speed up the convergence considerably.

NUMERICAL EXAMPLES

We test our data-space inversion scheme on the Marmousi model. Figure 11 shows the reflectivity and velocity model used for the Born modeling under the blended acquisition geometry. A total of 51 shots are modeled with a uniform spacing of 100 m, ranging from 4000 m to 9000 m. The receiver spread ranges from 4000 m to 9000 m with a 10 m sampling and is fixed for all shots. As in the previous example of the scattering model, we also simulate linear-time-delay and random-time-delay blended acquisition geometries. Figure 12(a) and Figure 12(b) show the corresponding blended gathers. In both cases, all 51 gathers are blended into one super-areal shot gather.

Figure 13 shows the local Hessian operators for the blended acquisition geometries at different spatial locations in the subsurface. Note that the Hessian operators are far from unitary and contain many non-negligible off-diagonal elements, which contribute to the crosstalk in the migrated images.

The migration and data-space LSI results are shown in Figure 14 and Figure 15. In the inversion results, a horizontal Laplacian operator that imposes horizontal continuities of the reflectivity is used as the regularization operator $\mathbf{A}$. For both blended acquisition geometries, migration produces poor images (Figure 14(a) and Figure 15(a)), which are seriously contaminated by crosstalk artifacts. The data-space LSI, on the contrary, successfully removes the crosstalk and we get good reconstruction of the reflectivity in the subsurface (Figure 14(b) and Figure 15(b)).

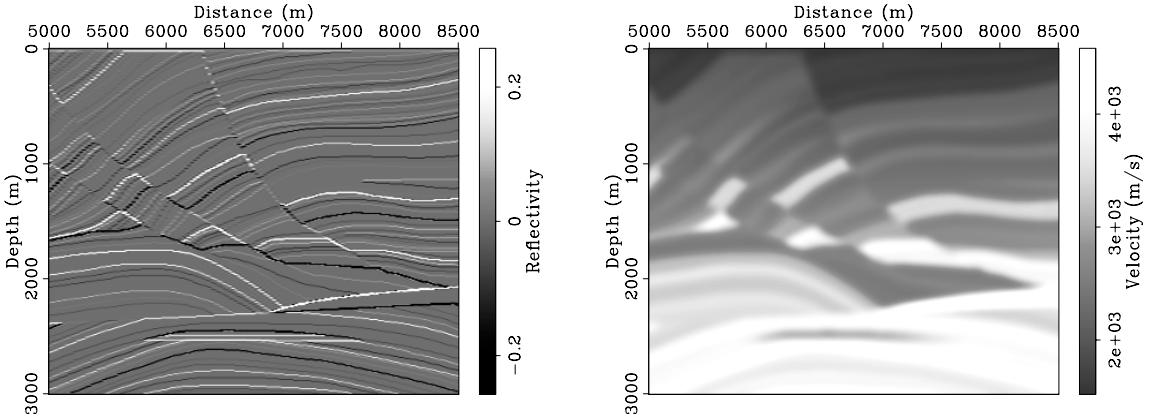

(a) (b)

Figure 11: The Marmousi model. (a) Reflectivity model; (b) background velocity model. [**ER**]

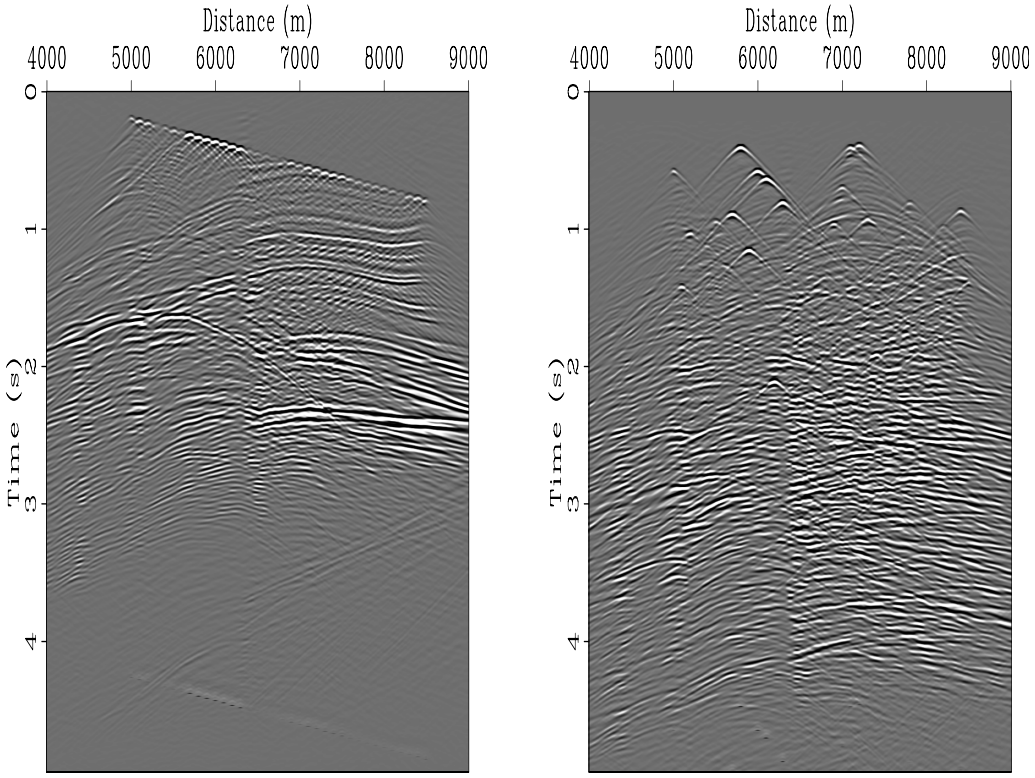

(a) (b)

Figure 12: Synthesized blended shot gather for (a) linear-time-delay blended acquisition and (b) random-time-delay blended acquisition. [**CR**]

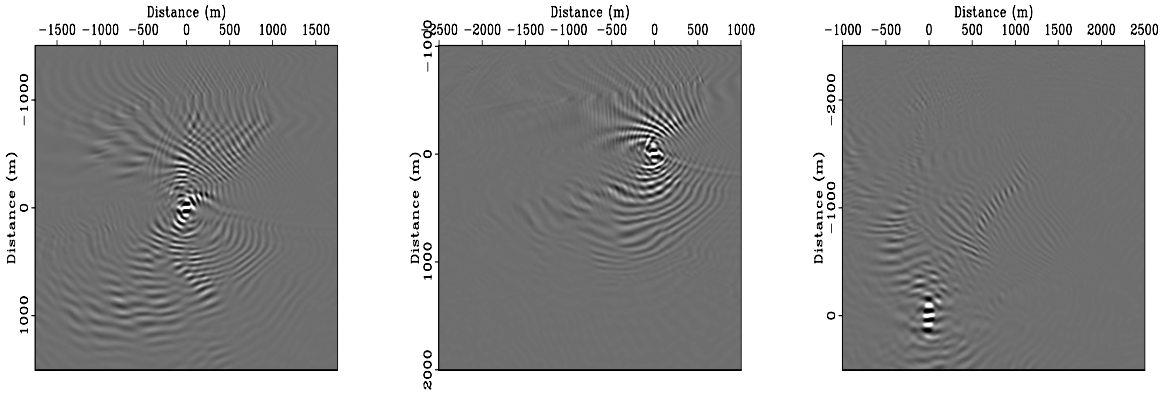

(a)

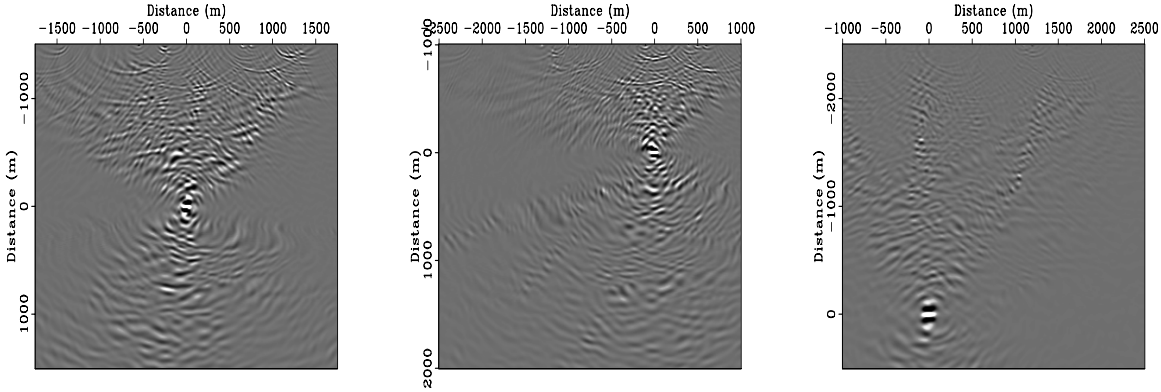

(b)

Figure 13: The local Hessian operators (rows of the full Hessian) at different locations for blended acquisition geometries. Panel (a) shows the results for linear-time-delay blending, while panel (b) shows the results for random-time-delay blending. In both (a) and (b), left, center and right panels are the local Hessians located at $x = 6750$ m, $z = 1500$ m; $x = 7500$ m, $z = 1000$ m; and $x = 6000$ m, $z = 2500$ m, respectively. [**CR**]

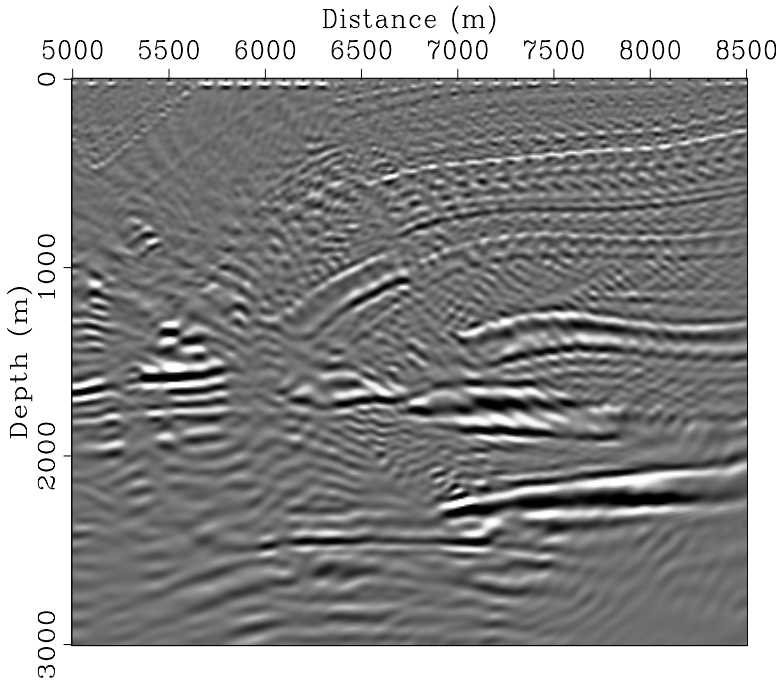

(a)

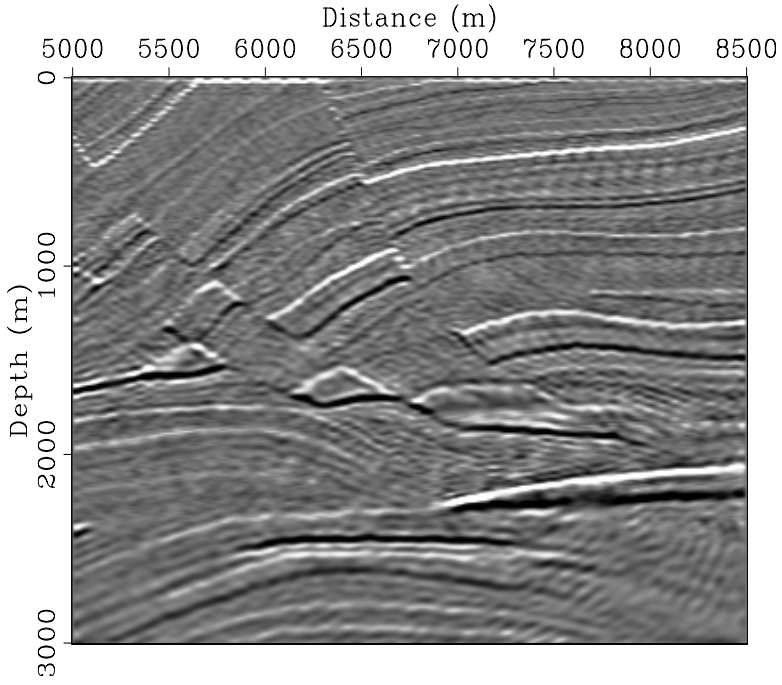

(b)

Figure 14: Comparison between (a) migration and (b) data-space LSI for the linear-time-delay blended acquisition geometry. [**CR**]

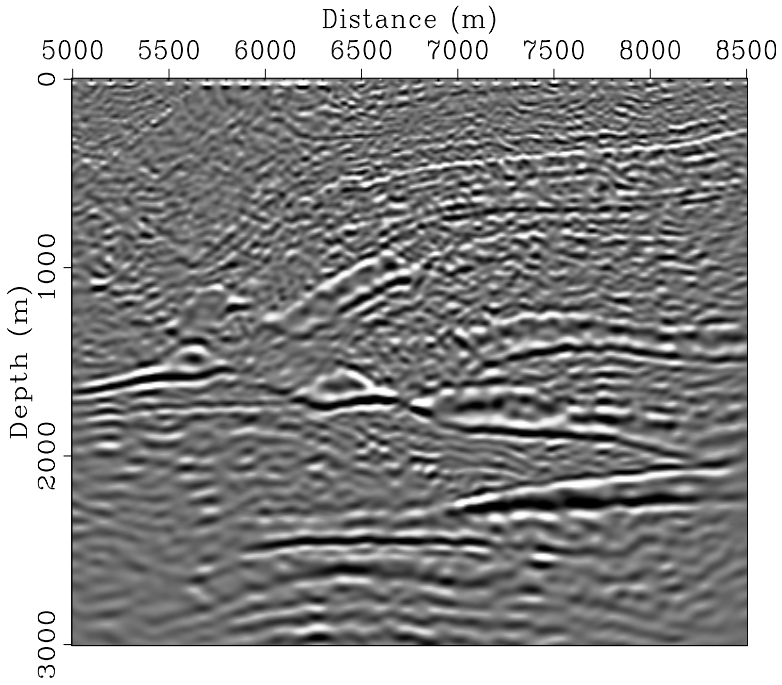

(a)

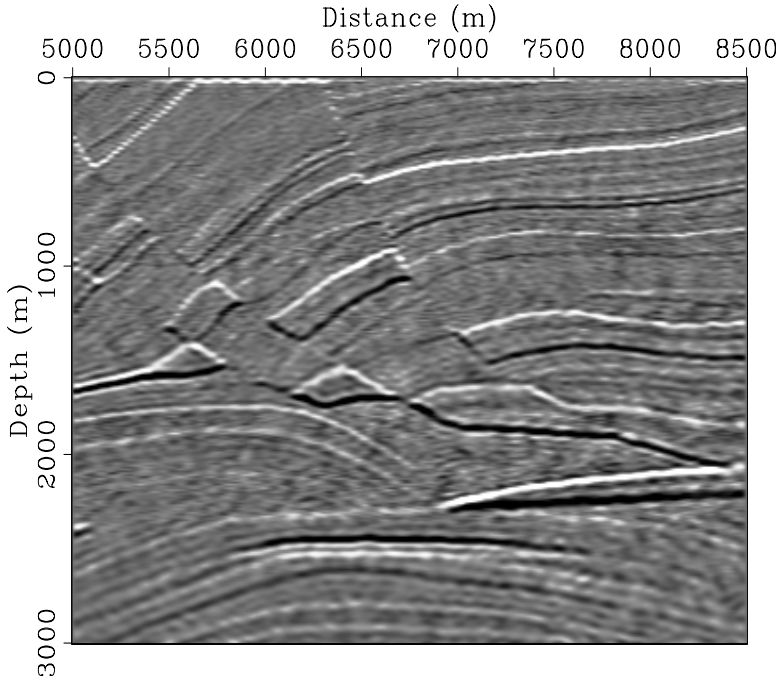

(b)

Figure 15: Comparison between (a) migration and (b) data-space LSI for the random-time-delay blended acquisition geometry. [**CR**]

DISCUSSION

Imaging through LSI in blended acquisition geometries is an underdetermined problem; hence there are an infinite number of solutions that fit the observed data equally well. Therefore, regularization is very important for constraining the corresponding solution. In the Marmousi example, a simple regularization operator that imposes horizontal smoothness seems to be working well. However, this choice may not be optimal, because it may wash out dipping reflectors. Regularization operators that better predict the inverse model covariance, for example, by imposing continuities along reflection angles and geological dips (Clapp, 2005), or promoting sparseness in the image domain (Tang, 2009), should be able to reduce the null space and further improve the inversion result. How to incorporate accurate prior information to constrain the inversion remains a research area for further investigation.

CONCLUSIONS

We present a method based on LSI to directly image the subsurface using blended data sets. This method does not require any pre-separation of the blended shot gathers, and the crosstalk is effectively removed by formulating the imaging problem as a least-squares inverse problem. The inversion examples on the Marmousi model show that LSI can successfully remove the crosstalk that migration generates and optimally reconstruct the reflectivity in the subsurface.

ACKNOWLEDGMENTS

We thank Guus Berkhout, whose invited talk at Stanford University inspired us to think about the potential opportunities of the blended acquisition geometry.

REFERENCES

Akerberg, P., G. Hampson, J. Rickett, H. Martin, and J. Cole, 2008, Simultaneous source separation by sparse radon transform: SEG Technical Program Expanded Abstracts, **27**, 2801–2805.

Ayeni, G., Y. Tang, and B. Biondi, 2009, Joint preconditioned inversion of simultaneous source time-lapse seismic data sets: SEG Technical Program Expanded Abstracts, **28**, submitted.

Beasley, C. J., 2008, A new look at marine simultaneous sources: The Leading Edge, **27**, 914–917.

Beasley, C. J., R. E. Chambers, and Z. Jiang, 1998, A new look at simultaneous sources: SEG Technical Program Expanded Abstracts, **17**, 133–135.

Berkhout, A. J. G., 2008, Changing the mindset in seismic data acquisition: The Leading Edge, **27**, 924–938.

Clapp, M. L., 2005, Imaging Under Salt: Illumination Compensation by Regularized Inversion: PhD thesis, Stanford University.

Hampson, G., J. Stefani, and F. Herkenhoff, 2008, Acquisition using simultaneous sources: The Leading Edge, **27**, 918–923.

Howard, M. S. and N. Moldoveanu, 2006, Marine survey design for rich-azimuth seismic using surface streamers: SEG Technical Program Expanded Abstracts, **25**, 2915–2919.

Keggin, J., T. Manning, W. Rietveld, C. Page, E. Fromyr, and R. van Borselen, 2006, Key aspects of multi-azimuth acquisition and processing: SEG Technical Program Expanded Abstracts, **25**, 2886–2890.

Michell, S., E. Shoshitaishvili, D. Chergotis, J. Sharp, and J. Etgen, 2006, Wide azimuth streamer imaging of mad dog; have we solved the subsalt imaging problem?: SEG Technical Program Expanded Abstracts, **25**, 2905–2909.

Nemeth, T., C. Wu, and G. Schuster, 1999, Least-squares migration of incomplete reflection data: Geophysics, **64**, 208–221.

Romero, L. A., D. C. Ghiglia, C. C. Ober, and S. A. Morton, 2000, Phase encoding of shot records in prestack migration: Geophysics, **65**, 426–436.

Spitz, S., G. Hampson, and A. Pica, 2008, Simultaneous source separation: A prediction-subtraction approach: SEG Technical Program Expanded Abstracts, **27**, 2811–2815.

Tang, Y., 2008a, Modeling, migration and inversion in the generalized source and receiver domain: **SEP-136**, 97–112.

———, 2008b, Wave-equation Hessian by phase encoding: SEG Technical Program Expanded Abstracts, **27**, 2201–2205.

———, 2009, Target-oriented least-squares migration/inversion with sparseness constraints: **SEP-138**.

Valenciano, A., 2008, Imaging by Wave-equation Inversion: PhD thesis, Stanford University.